Shahrekord University

Journal of Microfluidic and Nanofluidic Research

Journal homepage: https://jmnr.sku.ac.ir

Research Article

Effect of Fin Geometry on Entropy Generation in Heat Sink: A Numerical Investigation

Ahmad Najafpour *

Department of Mechanical Engineering, Babol Noshirvani University of Technology, Babol, Iran

ARTICLE INFO

Article history:

Received: 2025-05-08

Revised: 2025-06-21

Accepted: 2025-06-22

Keywords:

Entropy generation;

CFD;

Thermal performance;

Convection heat transfer

ABSTRACT

This study investigates the thermal performance and entropy generation of five mini-channel heat sink (MCHS) configurations under a constant heat flux of 50 kW/m^2. The heat sinks, made of copper with water as the working fluid, are analyzed over a Reynolds number range of 600–1400. The effects of different fin geometries on heat transfer, pressure drop, and entropy production are evaluated using numerical simulations in COMSOL Multiphysics. Results indicate that increasing the Reynolds number enhances convective heat transfer but also raises the pressure drop. Among the proposed designs, Case 2 demonstrates the most efficient performance, achieving the lowest entropy generation and superior cooling, in agreement with the second law of thermodynamics. These findings highlight the importance of fin geometry optimization for improving MCHS efficiency.

1. Introduction

In recent years, the growing need for smaller, faster, more powerful, and energy-efficient electronic devices has made thermal management a key factor in engineering design [1,2]. It is widely recognized that the heat produced by electronic components is closely linked to their operational efficiency. Therefore, designing advanced cooling solutions is essential to avoid thermal malfunction and maintain optimal performance [3,4]. Conventional cooling approaches are increasingly inadequate for managing the thermal challenges of modern high-power and miniaturized electronic systems. To enhance heat removal from such devices, a range of thermal management solutions has been explored, including passive air convection, liquid-based cooling, and advanced techniques like phase change materials [5,6]. Although these methods offer considerable benefits in numerous applications, they frequently fall short of the stringent thermal requirements of emerging compact and high-performance systems. In this regard, micro/mini-channel heat sinks (MCHSs) have attracted significant attention as efficient thermal control options. Their small-scale architecture and large surface-to-volume ratio enable superior heat dissipation, particularly when paired with liquid coolants [7- 9]. Owing to these advantages, MCHSs are now widely applied in high-power electronics, solar energy systems, and small-scale computing units. Depending on design and application, different coolants such as water, oils, and ethylene glycol are utilized, with liquid-based configurations typically achieving greater cooling efficiency because of their improved convective heat transfer behavior. Numerous investigations have aimed to improve the efficiency of microchannel heat sinks (MCHSs) by optimizing geometry, modifying

* **Corresponding author.**
E-mail address: amdnajafpour@gmail.com, amdnajafpour@stu.nit.ac.ir

Cite this article as:

Najafpour, A., 2025. Effect of Fin Geometry on Entropy Generation in Heat Sink: A Numerical Investigation. *Journal of Microfluidic and Nanofluidic Research*, 2(2), pp. 120-127. https://doi.org/10.22034/jmnr.2025.15497.1018

working fluids, and developing hybrid configurations.

Gunnasegaran et al. [10] analyzed triangular, rectangular, and trapezoidal microchannels each in three different sizes and reported that smaller hydraulic diameters led to higher heat transfer coefficients (HTCs) and better temperature uniformity, with rectangular geometries exhibiting the most favorable results. Likewise, Najafpour et al. [11] studied the influence of varying cross-sectional areas under Re between 831 and 1496, demonstrating that increasing the Re enhanced the HTC and decreased thermal resistance. The incorporation of nanoparticles such as TiO_2, MgO, and graphene oxide (GO) was also shown to improve heat dissipation by reducing both fluid temperature and overall thermal resistance relative to base water. In another work, Ghadhban and Jaffal [12] evaluated microchannels with wave, S-shaped, and arc geometries, finding notable gains in the Nusselt number up to 30.5% as well as a 16% decrease in ΔP for the arc-type configuration. Extending this line of research, Al-Hassani and Freegah [13] assessed serpentine microchannels featuring secondary flow variations, including backward angles, dual outlets, and pin-fin hybrid structures. Their findings indicated substantial improvements in Nusselt number and overall hydrothermal performance, though these benefits were accompanied by variations in ΔP. Najafpour et al. [14] introduced multi-branch microchannel layouts and analyzed their thermal behavior under a uniform heat flux of 26.67 kW/m^2. Out of the five proposed models, Case 2 exhibited the most optimal balance between heat transfer and flow resistance, showing a decrease in thermal resistance with increasing Re, albeit accompanied by a rise in pressure drop.

Despite notable progress in improving the thermal performance of microchannel heat sinks through modifications in geometry and coolant design, achieving an optimal compromise between heat transfer enhancement and pressure loss remains a persistent challenge. Numerous reported configurations enhance heat removal but simultaneously demand greater pumping power, thereby restricting their suitability for compact or energy-efficient systems. Moreover, the influence of fin configurations under moderate Re conditions, particularly when employing water as the working fluid and copper as the substrate, has not been comprehensively explored. The present work aims to bridge this research gap by analyzing various fin arrangements in a copper-based heat sink subjected to Re ranging from 600 to 1400 under a constant heat flux of 50 kW/m^2. The objective is to determine geometries that deliver improved thermal performance while maintaining an acceptable pressure drop value.

2. Numerical methodology

2.1. Geometric Shape and Boundary Conditions

In this study, five different mini-channel heat sink configurations are proposed, each with overall dimensions of 42 mm × 6 mm × 5 mm. The models consist of two solid copper domains and a fluid domain containing water, with the corresponding thermophysical properties summarized in Table 1.

Table 1. Material properties [7-9]

Material	Water	Copper
ρ (kg/m^3)	997	8933
c_p (J/kg.K)	4179	385
k (W/m.K)	0.6	401
μ (kg/m.s)	0.001	-

In all configurations, the heat sink base is exposed to a uniform heat flux of 50 kW/m^2. Each flow channel features a cross-sectional area of 2 mm × 2 mm, with the coolant entering at a constant temperature of 300 K. At the channel outlet, a zero-gauge pressure boundary condition is imposed, as illustrated in Fig. 1.

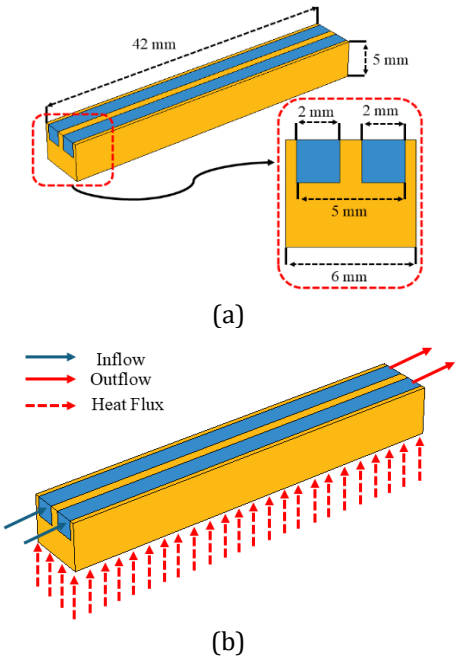

Fig. 1. (a) Geometric dimensions of the heat sink. (b)The boundary conditions.

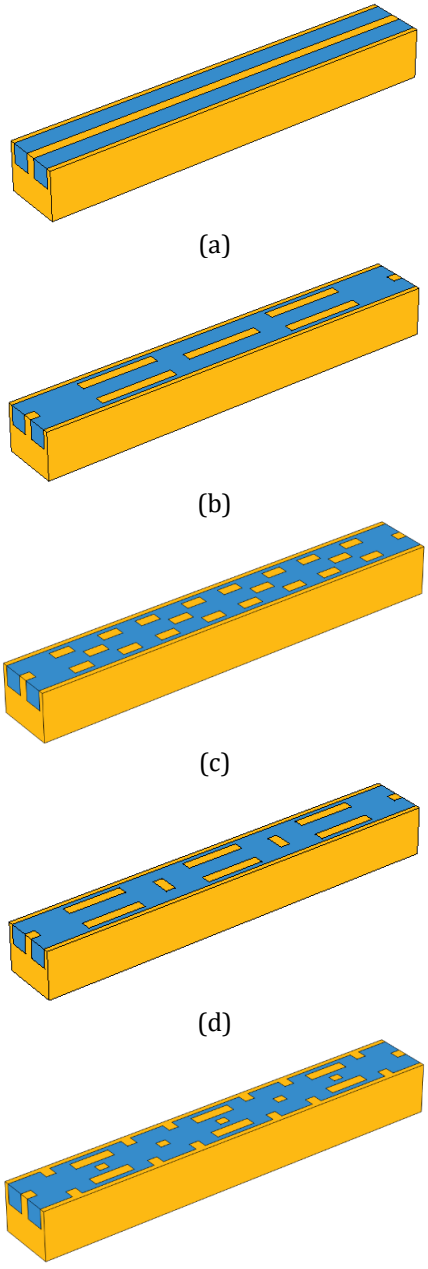

Fig. 2. Isometric view of ; a) base case, b) case 1, c) case 2, d) case 3 and e) case 4

The proposed configurations feature two inlets with a hydraulic diameter of D_h=2 mm, through which the coolant enters the flow channels at a constant temperature. After absorbing heat from the heated surface, the fluid exits through two outlets located at the downstream end of the channel. The simple model (Base Case) does not include any fins, whereas Cases 1 through 4 incorporate fins with distinct geometric arrangements designed to investigate the influence of fin shape variations on the cooling efficiency and overall thermal performance of the heat sink (Fig. 2). The presence of fins alters the flow distribution and enhances the convective surface area, enabling more effective heat transfer and temperature uniformity across the system.

2.2. Governing equations

To create a computational model that is both accurate and practical, several simplifying assumptions have been adopted. These assumptions reduce the mathematical complexity of the simulation while still adequately representing the fundamental physics of the problem. The modeling approach is built on the following primary considerations:

- The properties of the materials involved are assumed to be constant and not influenced by temperature changes during operation.
- The fluid flow is treated as laminar and incompressible, which is reasonable given the flow conditions considered.
- Phenomena like gravity and natural convection are disregarded, ensuring that the analysis concentrates solely on forced convection as the primary mode of heat transfer.
- A constant heat flux is imposed on the base of the heat sink to simulate a steady thermal load.
- Heat transfer by radiation is considered negligible and is thus omitted from the study.

Within these assumptions, the fluid flow and corresponding heat transfer are governed by the fundamental conservation equations: the continuity equation, the Navier–Stokes equations for momentum, and the energy equation.

The continuity equation is given as follows:

$$\frac{\partial u}{\partial x}+\frac{\partial v}{\partial y}+\frac{\partial w}{\partial z}=0 \quad (1)$$

Momentum equation:

$$u\frac{\partial u}{\partial x}+v\frac{\partial u}{\partial y}+w\frac{\partial u}{\partial z}=-\frac{1}{\rho_f}\frac{\partial p}{\partial x}+\frac{\mu_f}{\rho_f}\left[\frac{\partial^2 u}{\partial x^2}+\frac{\partial^2 u}{\partial y^2}+\frac{\partial^2 u}{\partial z^2}\right] \quad (2)$$

$$u\frac{\partial v}{\partial x}+v\frac{\partial v}{\partial y}+w\frac{\partial v}{\partial z}=-\frac{1}{\rho_f}\frac{\partial p}{\partial y}+\frac{\mu_f}{\rho_f}\left[\frac{\partial^2 v}{\partial x^2}+\frac{\partial^2 v}{\partial y^2}+\frac{\partial^2 v}{\partial z^2}\right] \quad (3)$$

$$u\frac{\partial w}{\partial x}+v\frac{\partial w}{\partial y}+w\frac{\partial w}{\partial z}=-\frac{1}{\rho_f}\frac{\partial p}{\partial z}+\frac{\mu_f}{\rho_f}\left[\frac{\partial^2 w}{\partial x^2}+\frac{\partial^2 w}{\partial y^2}+\frac{\partial^2 w}{\partial z^2}\right] \quad (4)$$

where p, ρ and ν denote the pressure, density, and kinematic viscosity of the coolant,

respectively. The energy equation for the fluid is formulated as follows:

$$u\frac{\partial T}{\partial x}+ v\frac{\partial T}{\partial y}+w\frac{\partial T}{\partial z}=\frac{k_f}{\rho_f c_{pf}}[\frac{\partial^2 T}{\partial x^2}+\frac{\partial^2 T}{\partial y^2}+\frac{\partial^2 T}{\partial z^2}] \quad (5)$$

Here, ρ, T, k_f, and Cp denote the coolant's density, temperature, thermal conductivity, and specific heat at constant pressure, respectively.

Energy equation for the solid:

$$k_s\left[\frac{\partial^2 T}{\partial x^2}+\frac{\partial^2 T}{\partial y^2}+\frac{\partial^2 T}{\partial z^2}\right]=0 \quad (6)$$

where k_s is the thermal conductivity of the solid.

2.3. Data Analysis

The value of ΔP can be concluded as follows [15, 16]:

$$\Delta P = P_{in} - P_{out} \quad (7)$$

The Re is a dimensionless quantity that is defined as follows:

$$Re = \frac{\rho U D_H}{\mu} \quad (8)$$

where D_H represents the hydraulic diameter of the flow channel, which is calculated using the following equation:

$$D_H = \frac{4A}{P} \quad (9)$$

Here, A denotes the cross-sectional area and P represents the perimeter of the fluid inlet.

This study employs the concept of entropy generation to assess heat transfer performance and flow irreversibilities in various MCHS configurations. The formulas for calculating the total entropy generation rates are presented below.

$$S_g = S_{g,\Delta p} + S_{g,\Delta T} \quad (10)$$

$$S_{g,\Delta p} = \frac{\dot{m}\Delta p}{\rho_m T_a} \quad (11)$$

$$S_{g,\Delta T} = \frac{Q_{base}\left(T_{base,avg} - T_a\right)}{T_{base,avg} T_a} \quad (12)$$

where $S_{g,\Delta T}$ accounts for entropy generation resulting from heat transfer, while $S_{g,\Delta p}$ represents entropy produced by the fluid motion. The fluid mass flow rate is denoted by $\dot{m}$ and the ambient temperature T_a is assumed to be identical to the inlet temperature in the present analysis.

The main purpose of the augmented entropy generation number, $N_{s,a}$ is to provide a means for comparing the irreversibility of different microchannel configurations. It is defined as follows [7, 8]:

$$N_{s,a} = S_g / S_{g,0} \quad (13)$$

Here, S_g represents the entropy generation for each configuration, which is evaluated relative to the baseline case using the formula in N_a. Values of N_a closer to zero indicate reduced entropy production and, therefore, improved cooling efficiency.

3. Grid Study and validation

In computational fluid dynamics (CFD) analyses, the precision and dependability of the results are strongly influenced by mesh quality. To ensure that the numerical outcomes are not overly sensitive to grid resolution, a mesh independence test was performed. This procedure allows an optimal trade-off between computational accuracy and processing cost, guaranteeing that the obtained data accurately represent the actual physical behavior. A four-step mesh independence assessment was conducted for Case 2 at a Re = 1000, focusing on ΔP and the base temperature of the heat sink. Based on the outcomes, a mesh containing approximately 1,834,283 elements was selected as adequate for the present simulations (Table 2). The governing equations of the current problem were discretized using the finite element method (FEM) implemented in COMSOL Multiphysics, where Equations 10^{-5} were solved considering all relevant parameters and boundary conditions.

Table 2. Mesh independence study.

Mesh	No.of elements	ΔP (Pa)	Bottom Tem (K)
1	402,465	1793.81	300.76
2	881,491	2253.71	301.65
3	**1,834.283**	**2938.44**	**301.89**
4	2,673,142	3050.59	301.93

To validate the accuracy of the present numerical approach, the obtained results were compared with the benchmark data reported by Al-Hasani and Freegah [13]. As depicted in Fig. 4, the outcomes from the current simulation show a close agreement with those of the reference study, with only minor deviations observed.

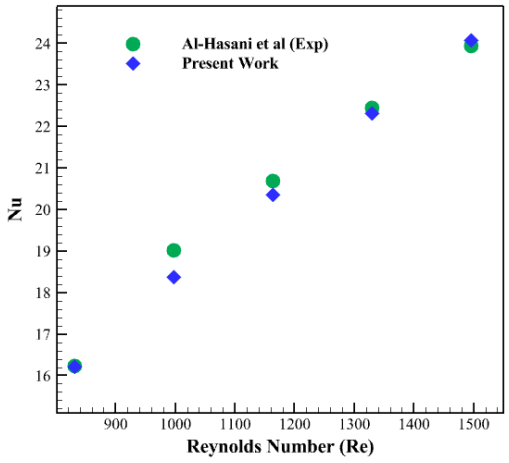

Fig. 3. Comparison of the results obtained with the numerical method compared to the work of Al-Hasani and Freegah [13].

4. Results and discussion

3.1. Impact of geometric design

Figure 5 presents the temperature contour distributions, illustrating the heat dispersion characteristics within the heat sink. In the baseline configuration, regions of elevated temperature appear due to restricted heat dissipation. By incorporating fins with varying geometrical arrangements in Cases 1-4, the temperature field becomes more uniform and significantly reduced. These fin designs increase the convective surface area and promote more effective fluid interaction with the heated zones, thereby enhancing thermal management and overall cooling performance.

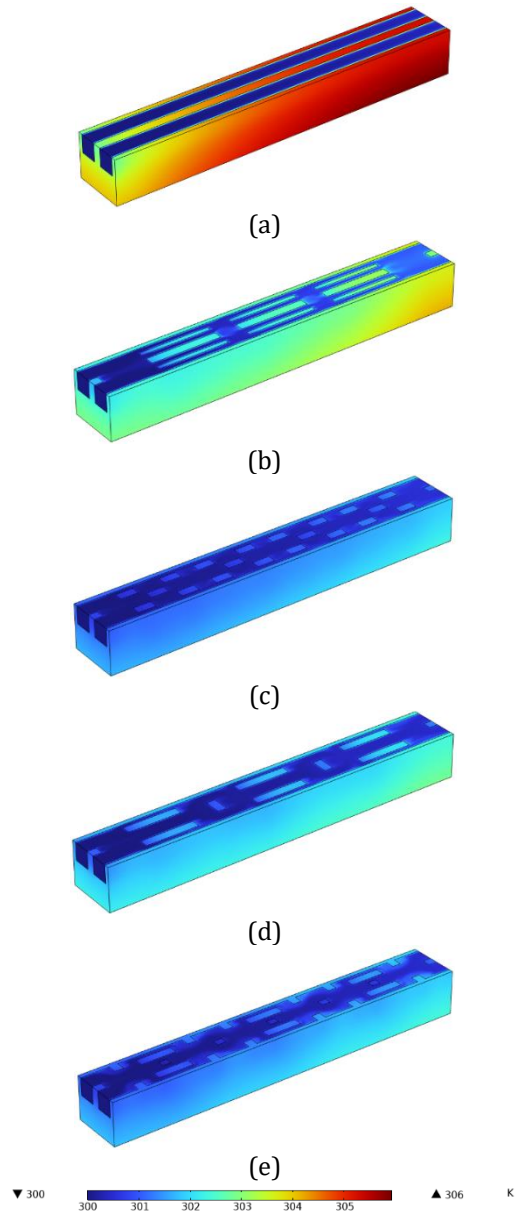

Fig. 4. Temperature distribution in present cases at a Re of 1000: (a) base case, (b) case 1, (c) case 2, (d) case 3, (e) case 4.

In Fig. 5 S_p graph shows the variation of the entropy production due to fluid friction with function of Re. As expected, increasing Re corresponds to higher flow velocities, which intensify the shear stress along the channel walls and thus increase the viscous losses. This results in more entropy production associated with fluid friction. All configurations show this general upward trend. However, the amount of entropy production varies among cases because the blade geometry affects the flow distribution, boundary layer thickness, and local velocity gradients. In particular, blade structures that provide better flow transfer tend to minimize viscous losses, while sharper or more complex geometries increase turbulence and increase frictional irreversibility.

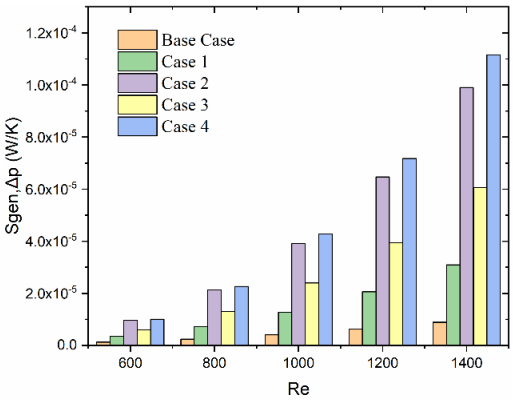

Fig. 5. S_p values for proposed cases at Re = 600 to 1400.

In Fig. 6 St diagram demonstrates that an increase in Re enhances the overall cooling capability and heat transfer efficiency of the system. As the Re rises from 600 to 1400, the fluid velocity correspondingly increases, resulting in a thinner thermal boundary layer and more effective convective heat transfer between the coolant and the channel walls. Consequently, the temperature difference between the working fluid and the heat sink surface diminishes, indicating improved thermal uniformity. This enhancement in heat removal also leads to higher entropy generation associated with heat transfer, as a greater temperature gradient is maintained across the fluid domain. The observed trend highlights the influence of fin geometry on thermal performance, emphasizing that optimized fin arrangements can maximize convective efficiency while maintaining balanced entropy production and ΔP. Case 4 has the lowest ST values, so that at a Re = 1000, the ST value in Case 4 has decreased by 60.98% and 31.98% compared to the base case and Case 1.

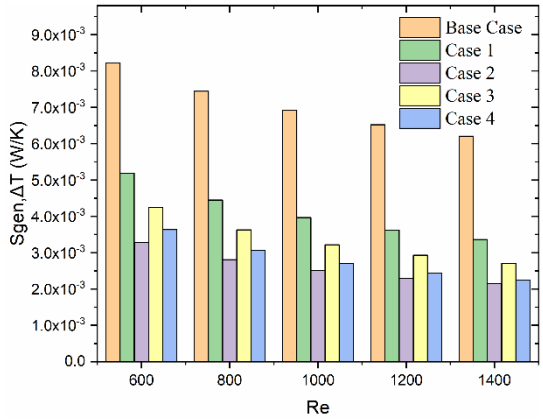

Fig. 6. S_t values for proposed cases at Re = 600 to 1400

In Fig 7 presents the variation of the Na parameter for Cases 1 to 4 in comparison with the baseline configuration. A lower Na value signifies reduced thermodynamic irreversibility and thus superior performance based on the second law of thermodynamics. In this regard, configurations exhibiting smaller Na values are considered more efficient, as they minimize entropy generation and utilize the available energy more effectively. This reduction in irreversibility reflects a better balance between heat transfer enhancement and frictional losses, indicating that optimized fin arrangements can improve exergy efficiency by promoting more orderly energy conversion within the heat sink system. The results show that Case 4 has the best performance among the proposed cases, so that at Re of 600 and 1400, Case 4 has improved by 55.71% and 61.99% compared to the base case. Case 3 has improved by 51.14% and 54.53% at Re = 800 and 1200, compared to the simple case.

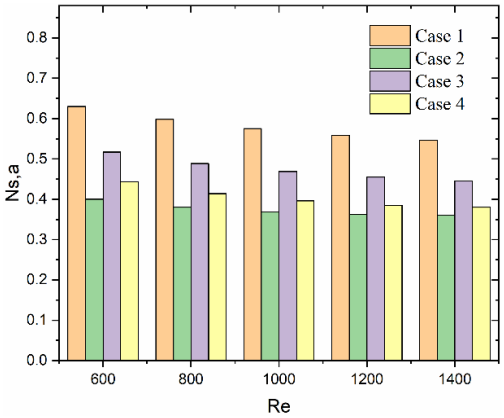

Fig. 7. N_a values for proposed cases at Re = 600 to 1400.

5. Conclusions

This study investigated five different heat sink configurations subjected to a constant heat flux of 50 kW/m2. The thermal performance and entropy generation were evaluated over the Re range of 600 to 1400. The results showed that increasing Re leads to increasing Sp and decreasing St. Among the cases, Case 2 shows the lowest entropy generation, which is consistent with the second law of thermodynamics. The main findings of this study are summarized as follows.

- Case 4 has the lowest ST values, so that at a Re = 1000, the ST value in Case 4 has decreased by 60.98% and 31.98% compared to the base case and Case 1.
- The results show that Case 4 has the best performance among the proposed cases, so that at Re of 600 and 1400, Case 4 has improved by 55.71% and 61.99% compared to the base case.
- Case 3 is improved by 51.14% and 54.53% at Re of 800 and 1200 compared to the simple case.

Nomenclature

Re	Reynolds Number
D_h	Hydraulic Diameter [m]
ΔP	Pressure Drop [Pa]
P	Pressure [Pa]
u	Velocity in x direction [m/s]
v	Velocity in y direction [m/s]
w	Velocity in z direction [m/s]
ρ	Density [kg/m^3]
c_p	Heat Transfer Capacity [J/kg.K]
k	Thermal Conductivity [W/m.K]
S_p	Entropy generation due to fluid flow (W/K)
S_t	Entropy generation due to heat transfer (W/K)
N_a	Entropy generation number

References

[1] He, Z., Yan, Y., & Zhang, Z., 2021. Thermal management and temperature uniformity enhancement of electronic devices by micro heat sinks: A review. Energy, 216, p. 119223.

[2] Hajialibabaei, M., Saghir, M.Z., 2022, A critical review of the straight and wavy microchannel heat sink and the application in lithium-ion battery

thermal management. International Journal of Thermofluids, 14, p. 100153.

[3] Hu, X., Gong, X., Zhu, F., Xing, X., Li, Z., Zhang, X., 2023, Thermal analysis and optimization of metal foam PCM-based heat sink for thermal management of electronic devices. Renewable Energy, 212, pp. 227-237.

[4] Akula, R., Balaji, C., 2022, Thermal management of 18650 Li-ion battery using novel fins–PCM–EG composite heat sinks. Applied Energy, 316, p. 119048.

[5] Wang, R., Liang, Z., Souri, M., Esfahani, M. N., Jabbari, M., 2022, Numerical analysis of lithium-ion battery thermal management system using phase change material assisted by liquid cooling method. International Journal of Heat and Mass Transfer, 183, p. 122095.

[6] Tyagi, V.V., Chopra, K., Kalidasan, B., Chauhan, A., Stritih, U., Anand, S., Kothari, R., 2021, Phase change material based advance solar thermal energy storage systems for building heating and cooling applications: A prospective research approach. Sustainable Energy Technologies and Assessments, 47, p. 101318.

[7] Najafpour, A., Ranjbar, A. A., Ganji, D. D., Hosseinzadeh, K., 2025, Entropy Generation and Thermal Analysis of Geometrically Modified Heat Sinks with Ternary Nanofluids. Case Studies in Thermal Engineering, p. 106713.

[8] Najafpour, A., Hosseinzadeh, K., Hasibi, A., Ranjbar, A. A., Ganji, D.D., 2025, Entropy Based Optimization of Mini-Channel Heat Sinks with Advanced Ternary Nanofluids for Photovoltaic Cells and Geometrical Enhancements. Results in Engineering, p. 104982

[9] Najafpour, A., Rostami, M.H., 2025, Numerical analysis of thermal and hydrothermal characteristics of a heat sink with various fin configurations and ternary nanofluid composition. Case Studies in Thermal Engineering, 68, p. 105928.

[10] Gunnasegaran, P., Mohammed, H.A., Shuaib, N.H., Saidur, R., 2010, The effect of geometrical parameters on heat transfer characteristics of microchannels heat sink with different shapes. International Communications in Heat and Mass Transfer, 37(8), pp. 1078-1086.

[11] Najafpour, A., Hosseinzadeh, K., Kermani, J.R., Ranjbar, A.A., Ganji, D.D., 2024, Numerical study on the impact of geometrical parameters and employing ternary hybrid nanofluid on the hydrothermal performance of mini-channel heat sink. Journal of Molecular Liquids, 393, p. 123616.

[12] Ghadhban, F.N., Jaffal, H.M., 2023, Numerical investigation on heat transfer and fluid flow in a multi-minichannel heat sink: Effect of channel configurations. Results in Engineering, 17, p. 100839.

[13] Al-Hasani, H.M., Freegah, B., 2022, Influence of secondary flow angle and pin fin on hydro-thermal evaluation of double outlet serpentine mini-channel heat sink. Results in Engineering, 16, p. 100670.

[14] Najafpour, A., Montazer, E., Hosseinzadeh, K., Ranjbar, A.A., Ganji, D.D., Kanesan, J., 2024, Computational study on the impact of geometric parameters on the overall efficiency of multi-branch channel heat sink in the solar collector. International Communications in Heat and Mass Transfer, 158, p. 107884.

[15] Najafpour, A., Akbari, S., Hosseinzadeh, K., Bijarchi, M. A., Ranjbar, A. A., Ganji, D.D., 2025, Active 3D electro-osmotic control micromixers: Effects of geometry, DC, and AC electric fields on mixing performance. International Communications in Heat and Mass Transfer, 165, p. 109033.

[16] Bayareh, M., Najafpour, A., 2025, Mixing intensification of an electroosmotic micromixer with circular mixing units and constriction channels. Chemical Engineering and Processing-Process Intensification, p. 110557.